Environ Monit Assess (2013) 185:4591–4603
DOI 10.1007/s10661-012-2890-8

Fluorescence spectroscopic characterization of dissolved organic matter fractions in soils in soil aquifer treatment

Shuang Xue · Qingliang Zhao · Liangliang Wei · Youtao Song · Mei Tie

Received: 21 November 2011 / Accepted: 11 September 2012 / Published online: 28 September 2012

Abstract This work investigated the effect of soil aquifer treatment (SAT) operation on the fluorescence characteristics of dissolved organic matter (DOM) fractions in soils through laboratory-scale soil columns with a 2-year operation. The resin adsorption technique (with XAD-8 and XAD-4 resins) was employed to characterize the dissolved organic matter in soils into five fractions, i.e., hydrophobic acid (HPO-A), hydrophobic neutral (HPO-N), transphilic acid (TPI-A), transphilic neutral (TPI-N), and hydrophilic fraction (HPI). The synchronous fluorescence spectra revealed the presence of soluble microbial byproduct- and humic acid-like components and polycyclic aromatic compounds in DOM in soils, and SAT operation resulted in the enrichment of these fluorescent materials in all DOM fractions in the surface soil (0–12.5 cm). More importantly, the quantitative method of fluorescence regional integration was used in the analysis of excitation–emission matrix (EEM) spectra of DOM fractions in soils. The cumulative EEM volume ($\Phi_{T,\,n}$) results showed that SAT operation led to the enrichment of more fluorescent components in HPO-A and TPI-A, as well as the dominance of less fluorescent components in HPO-N, TPI-N, and HPI in the bottom soil (75–150 cm). Total $\Phi_{T,\,n}$ values, which were calculated as $\Phi_{T,n} \times DOC$, suggested an accumulation of fluorescent organic matter in the upper 75 cm of soil as a consequence of SAT operation. The distribution of volumetric fluorescence among five regions (i.e., $P_{i,\,n}$) results revealed that SAT caused the increased content of humic-like fluorophores as well as the decreased content of protein-like fluorophores in both HPO-A and TPI-A in soils.

Keywords Soil aquifer treatment · Dissolved organic matter · Fluorescence spectroscopy · Soil · Fractionation

S. Xue · Y. Song · M. Tie
School of Environmental Science, Liaoning University, Shenyang 110036, China

S. Xue · Y. Song (✉) · M. Tie
Key Laboratory of Water Environment Biomonitoring and Ecological Security of Liaoning Province, Shenyang 110036, China
e-mail: shuangxue_777@163.com

Q. Zhao · L. Wei
School of Municipal and Environmental Engineering, Harbin Institute of Technology, Harbin 150090, China

Q. Zhao
State Key Laboratory of Urban Water Resources and Environments, Harbin Institute of Technology, Harbin 150090, China

Abbreviations

CEC	Cation exchange capacity
CS1	The soil at depths of 0–12.5 cm in the soil columns
CS2	The soil at depths of 12.5–25 cm in the soil columns
CS3	The soil at depths of 25–50 cm in the soil columns

CS4	The soil at depths of 50–75 cm in the soil columns
CS5	The soil at depths of 75–100 cm in the soil columns
CS6	The soil at depths of 100–125 cm in the soil columns
CS7	The soil at depths of 125–150 cm in the soil columns
DOC	Dissolved organic carbon
DOM	Dissolved organic matter
EC	Electrical conductivity
EEM	Excitation-emission matrix
Em	Emission wavelength
Ex	Excitation wavelength
FRI	Fluorescence regional integration
HPI	Hydrophilic fraction
HPO-A	Hydrophobic acid
HPO-N	Hydrophobic neutral
OS	The original homogenized soil used to pack the soil columns
SAT	Soil aquifer treatment
SMP	Soluble microbial byproduct
SOC	Soil organic carbon
TPI-A	Transphilic acid
TPI-N	Transphilic neutral
$\Phi_{i\,n}$	Normalized region-specific EEM volume
$\Phi_{T\,n}$	Cumulative EEM volume
$P_{i\,n}$	Percent fluorescence response

Introduction

Soil aquifer treatment (SAT) represents a wastewater reclamation technology that can renovate wastewater effluent to drinking water levels, and hence can be an important component in an indirect potable reuse system (Amy and Drewes 2007). Organic matter is a major water quality issue during SAT, as organic carbon present in recovered groundwater can negatively interfere with subsequent treatment operations contributing to disinfection by-product formation, membrane fouling, or biological regrowth in distribution systems (Rauch and Drewes 2005). Organic matter present in wastewater effluent is removed by a combination of biological, chemical, and physical process in the vadose zone and subsequently in the aquifer (Quanrud et al. 1996). The majority of organic matter reduction was attained within meters of the surface soil (Quanrud et al. 1996; Westerhoff and Pinney 2000; Quanrud et al. 2003; Xue et al. 2009).

Dissolved organic matter (DOM) in soils is known to play various ecological roles, because DOM is the link between the geosphere and the hydrosphere, as well as the link between the biosphere and the non-biosphere (Akagi et al. 2007). Therefore, this most labile and reactive fraction of the multi-component soil organic matter pool, even though it typically constitutes less than 1 % of total organic matter (Ohno et al. 2007), may most rapidly reflect changes in the condition of a soil (Akagi et al. 2007). Although a number of studies in the past reported the fate and transport of DOM present in infiltrated water during SAT, the effect of SAT on organic matter in soils has so far received much less attention. Fox et al. (2005) found that the accumulation of organic matter in the top 8 cm of soil was <20 % of the total organic matter applied to the columns and soils at depths greater than 8 cm had total organic matter levels less than the original soils before soil aquifer treatment, through column and field studies. Quanrud et al. (1996) observed no increase in soil organic carbon (SOC) occurred below a depth of 8 cm in laboratory-scale soil columns after 11 months of SAT operation. However, the effect of SAT on DOM in soils remains unclear.

DOM consists of a continuum of macroscopic particles, biotic and abiotic colloids, dissolved macromolecules, and specific compounds (Barber et al. 2001). Owing to the important role played by DOM in mobility and fate of plant nutrients, regulation, and environmental contaminants, it is particularly useful to better characterize them (Chen et al. 2003a). Among analytical characterization methods, fluorescence spectroscopy appears to be most useful because of its ability to provide information on the chemical properties of the fluorescing fraction of organic matter coupled with its high sensitivity that allows analysis at low native DOM concentrations (Leenheer and Croué 2003). Fluorescence characteristics are selective for changing chemical components based on the closely spaced molecular energy levels unique to each component's chemical structure and its concentration in solution (Boehme et al. 2004). This sensitivity enables the characterization of structural changes as the chemical environment changes, as well as the interaction of the fluorophore with its surrounding components (Ohno et al. 2007). Various fluorescence spectroscopy techniques have been used to characterize DOM,

including emission, excitation–emission matrix (EEM), and synchronous scan excitation techniques (Chen et al. 2003b).

EEM fluorescence spectroscopy is well suited to analyze a mixture of fluorophores of unknown spectral properties, utilizing multiple excitation and emission wavelengths with intensity to examine total luminescence characteristics (Boehme et al. 2004). Fluorescence regional integration (FRI), a quantitative technique that integrates the volume beneath an EEM, was proposed by Chen et al. (2003b) to quantify multiple broad-shaped EEM peaks. EEM spectra were divided in five excitation–emission regions using consistent excitation and emission wavelength boundaries, and the quantitative analysis included the integration of the volume beneath each region, which represents the cumulative fluorescence response of DOM with similar properties (Chen et al. 2003b). The FRI technique is used to analyze quantitatively all the wavelength-dependent fluorescence intensity data from EEM spectra (Marhuenda-Egea et al. 2007).

Synchronous fluorescence spectroscopy offers a potentiality to reduce overlapping interferences and a possibility for each fluorescent component to be identified in a specific spectral range (Peuravuori et al. 2002). Synchronous scan excitation spectra are obtained by measuring the fluorescence intensity while simultaneously scanning over both the excitation and emission wavelengths while keeping a constant wavelength interval $\Delta\lambda$ between them (Chen et al. 2003a; Sierra et al. 2005).

The main purpose of this study was to reveal changes in the fluorescence characteristics of soil DOM in SAT systems through laboratory-scale soil columns with a 2-year operation. Due to its heterogeneity, the structural and functional characterization of DOM is extremely challenging. The fractionation of the bulk DOM into some well-defined subcomponents has been reported to offer advantages in characterizing DOM and providing improved understanding of the structural and functional properties of DOM. In this study, DOM, which was extracted from the original soil used to pack the soil columns and from soils at different depths in the soil columns after a 2-year SAT operation, was subjected to DOM fractionation procedure. The DOM fractionation method used in this study is based on methods following Aiken et al. (1992) and Chow et al. (2006). Accordingly, DOM was separated into five fractions which are operationally defined as: hydrophobic acid (HPO-A) reversibly adsorbed onto XAD-8 resin at pH 2 and dissolved during back elution of XAD-8 resin with 0.1 mol/L NaOH, hydrophobic neutral (HPO-N) reversibly adsorbed onto XAD-8 resin at pH 2 and not dissolved during back elution of XAD-8 resin with 0.1 mol/L NaOH, transphilic acid (TPI-A) reversibly adsorbed onto XAD-4 resin at pH 2 and dissolved during back elution of XAD-4 resin with 0.1 mol/L NaOH, transphilic neutral (TPI-N) reversibly adsorbed onto XAD-4 resin at pH 2 and not dissolved during back elution of XAD-4 resin with 0.1 mol/L NaOH, and hydrophilic fraction (HPI) that passes through both XAD-8 and XAD-4 resins. And then the EEM and synchronous scan excitation techniques, as well as the FRI analysis were employed to examine the fluorescence properties of DOM fractions. The results of this study may be important for the operation of SAT systems and groundwater resources management. During SAT, sorption to soils followed by microbial degradation is the most important removal mechanisms for organics present in infiltrated waters. Especially for those relatively resistant to biodegradation, sorption is most likely a limiting step for their removal during SAT, as attachment to soil surfaces may increase their availability for bacteria (Juhna et al. 2003). DOM in soils has a strong influence on these reactions and processes during SAT. Besides its function as substrate for microorganisms, it is well known that solubility and transport of organic contaminants as well as heavy metals through soils are linked to DOM properties. Also, a large number of important soil properties and functions are directly linked to the amount and quality of DOM (Embacher et al. 2007). Furthermore, DOM in soils forms a potential source of organic matter for infiltrated waters, which reacts with chlorine to form carcinogenic disinfection by-products during chlorination for reuses (Westerhoff and Pinney 2000). These in turn play a significant role in the performance of SAT systems and water quality of SAT product waters. Hence, a better understanding of the structural and functional properties of DOM in soils resulted from the DOM fractionation technique and fluorescence spectroscopy in this study may greatly improve our understanding of the underlying mechanisms responsible for the complexation, reduction, and mobilization or immobilization of heavy metals and toxic organic contaminants with DOM (Chen et

al. 2003a). This may improve our predictive capabilities of the behavior of DOM and environmental pollutants in SAT systems, and, in turn, may facilitate the pretreatment and posttreatment choices as well as water quality control for SAT systems.

Materials and methods

Soil sampling and characterization

In order to study changes of DOM in soils during SAT, a laboratory-scale SAT system which consisted of three soil columns was developed and operated for a period of 2 years. The operation of the SAT system and characteristics of SAT-applied wastewater effluents were described in detail in Xue et al. (2007). After operation of this system was terminated, soil was obtained from the columns and divided into seven subsamples (CS1–CS7) of 12.5/25 cm increments. The sample of the original homogenized soil (OS) used to pack the columns was also analyzed to determine the effects of SAT. Soil samples were air-dried, manually ground, and sieved to <2 mm before analysis. Soil pH and electrical conductivity (EC) were measured on a 1:1 soil/water mixture, according to US Environmental Protection Agency (EPA) Methods 9045C and 9050, respectively. Soil cation exchange capacity (CEC) was determined according to EPA method 9081. SOC was measured by $K_2Cr_2O_7$ digestion (Method of Soil Analysis, 1989). Chemical characteristics of these soil samples are shown in Table 1.

Table 1 Chemical characteristics of soil samples used in this study

Soil	Depth (cm)	pH	EC (μS/cm)	CEC (cmol/kg)	SOC (mg/g)
OS	–	8.2	1,915	7.3	29.3
CS1	0–12.5	7.2	955	8.9	36.7
CS2	12.5–25	6.7	1,000	13.1	26.9
CS3	25–50	7.1	990	6.9	25.5
CS4	50–75	6.9	952	9.2	26.2
CS5	75–100	7.0	1,072	7.8	25.4
CS6	100–125	6.8	1,390	10.4	25.1
CS7	125–150	6.9	1,133	11.6	25.2

DOM extraction

One hundred grams of dry soil were mixed with 1,000 ml of ultra-pure water (Milli-Q) in a 2-L glass container to prepare a 1:10 (*w*/*v*) extraction. The soil suspension was stirred for 2 h at about 20 °C. Afterwards, the suspension was transferred to a glass centrifuge tube and centrifuged at 250×*g* relative centrifugal force for 20 min. The supernatant was withdrawn and filtered using 0.45-μm cellulose nitrate membrane filter on a vacuum system. The water extracts were stored in a freezer until further analyses.

DOM fractionation

DOM fractionation was performed in duplicate for each sample. The steps were as follows: (1) acidify 0.45-μm filter-filtered water extracts to pH 2 with 6 mol/L HCl, pass the acidified sample through two columns in series containing XAD-8 and XAD-4 resins using a peristaltic pump with Tygon tubing at a flow rate of about 1 mL/min, then rinse the columns with 1 bed volumes of 0.01 mol/L HCl. HPI is the carbon in the XAD-4 effluent; (2) elute each column separately in the reverse direction with 3 bed volumes of 0.1 mol/L NaOH, followed by 3 bed volumes of Milli-Q water, at a flow rate not exceeding 0.5 mL/min. The eluate from XAD-8 is defined as HPO-A and the eluate from XAD-4 is defined as TPI-A. Both HPO-A and TPI-A were desalted using cation exchange resin; and (3) elute each column separately with 3 bed volumes of 75 % acetonitrile/25 % Milli-Q water solution at a flow rate of about 1 mL/min. The eluates from XAD-8 and from XAD-4 are defined as HPO-N and TPI-N, respectively. Acetonitrile was subsequently removed using rotary-evaporation.

Analysis

Dissolved organic carbon (DOC) concentration for DOM fractions was analyzed using a Shimadzu TOC-5000 Total Organic Carbon Analyzer with auto-sampler.

Fluorescence spectra were obtained with a JASCO FP-6500 spectrofluorometer. The spectrofluorometer used a Xenon excitation source, and slits were set to 5 nm for both excitation and emission. Filtered water extracts were diluted to 1 mg/L of DOC with 0.01 mol/L KCl, and acidified to pH 3 with HCl to

minimize complexation of metals with DOC (Drewes et al. 2006). The emission wavelength (Em) range was fixed from 290 to 550 nm (1-nm intervals), whereas the excitation wavelength (Ex) was increased from 220 to 400 nm (5-nm intervals). Scan speed was set at 1,000 nm/min, generating an EEM in about 15 min. Synchronous scan excitation spectra were recorded with the excitation monochromator scanned from 260 to 550 nm and $\Delta\lambda$=60 nm. The wavelength step size was 1 nm. Blank sample (0.01 mol/L KCl at pH 3) fluorescence was subtracted form all spectra.

Statistical analyses were conducted using SPSS version 13.0 (SPSS Inc., Chicago, IL, USA), with p <0.05 used as the criterion for statistical significance.

Results and discussion

FRI parameters

EEM spectra for DOM fractions extracted from the original soil used to pack the soil columns and from soils at different depths in the soil columns after a 2-year SAT operation are shown in Fig. 1. To analyze quantitatively EEM spectra, EEM spectra were divided into five regions using consistent excitation and emission wavelength boundaries (Fig. 1). The five regions were as follows: regions I (Ex 220–250 nm–Em 290–330 nm) and II (Ex 220–250 nm–Em 330–380 nm) recognized as belonging to aromatic protein-like fluorescence; region III (Ex 220–250 nm–Em 380–550 nm) associated with fulvic acid-like fluorescence; region IV (Ex 250–400 nm–Em 290–380 nm) related to soluble microbial byproduct-like (SMP-like) florescence; and regionV (Ex 250–400 nm–Em 380–550 nm) assigned to humic acid-like fluorescence (Chen et al. 2003b; Marhuenda-Egea et al. 2007).

The quantitative analysis of EEMs was conducted following the FRI technique proposed by Chen et al. (2003b), which integrate the volume beneath EEM spectra. According to Chen et al. (2003b), normalized region-specific EEM volume ($\Phi_{i,n}$), cumulative EEM volume ($\Phi_{T,n}$), and percent fluorescence response ($P_{i,n}$) were calculated as follows:

$$\Phi_{i,n} = \mathrm{MF}_i \Phi i \tag{1}$$

$$\Phi_{T,n} = \sum \Phi_{i,n} \tag{2}$$

$$P_{i,n} = \Phi_{i,n} / \Phi_{T,n} \times 100\% \tag{3}$$

Where Φ_i is the volume beneath region "i" of the EEM and MF_i is the multiplication factor for each region, which was equal to the inverse of the fractional projected excitation–emission area (Table 2).

In this study, the blank-subtraction procedure, i.e., subtracting the EEM of Milli-Q water blank from that of the water sample, was used to eliminate the Raman scattering interference. However, this procedure was unable to completely eliminated Rayleigh scattering, which can be problematic when analyzing water samples with low-colored dissolved organic matter concentrations (Zepp et al. 2004). To eliminate the Rayleigh scattering interference, the intensity values at points where the emission wavelength was the same as or twice the excitation wavelength, as well as those adjacent to them (±10 nm emission wavelength at the same excitation wavelength), were excised from the scan data and the excised values were replaced with zero (Xiao et al. 2010). In addition, this procedure was also applied to the data points in EEMs with an emission wavelength < the excitation wavelength or > twice the excitation wavelength. All data points whose value had been replaced with zero were excluded when counting the number of EEM data points per region and subsequently calculating projected excitation–emission area and MF_i (Table 2).

FRI analysis of DOM fractions in soils in SAT

The $\Phi_{\mathrm{I},n}$–$\Phi_{\mathrm{V},n}$, and $\Phi_{T,n}$ values for HPO-A, HPO-N, TPI-A, TPI-N, and HPI in the pre-SAT soil and seven post-SAT soil layer samples were present in Fig. 2. All $\Phi_{i,n}$ and $\Phi_{T,n}$ values shown in Fig. 2 were normalized to a DOC concentration of 1 mg/L for comparison of EEMs of these DOM fractions. For each DOM fraction, $\Phi_{i,n}$ was significantly different (p<0.05) among these five fluorescence regions. Also, the $\Phi_{i,n}$ for each region, as well as $\Phi_{T,n}$, was different (p<0.05) among DOM fractions. The increase in $\Phi_{T,n}$ value is an indication for the enrichment of more fluorescent components in soil DOM fractions as a result of SAT operation. Such increase was observed for both HPO-A and TPI-A, showing an increase of 6–173 % and 6–218 % for all soil samples obtained from the laboratory-scale SAT columns (CS1–CS7) relative to the original soil before SAT (OS), respectively. In

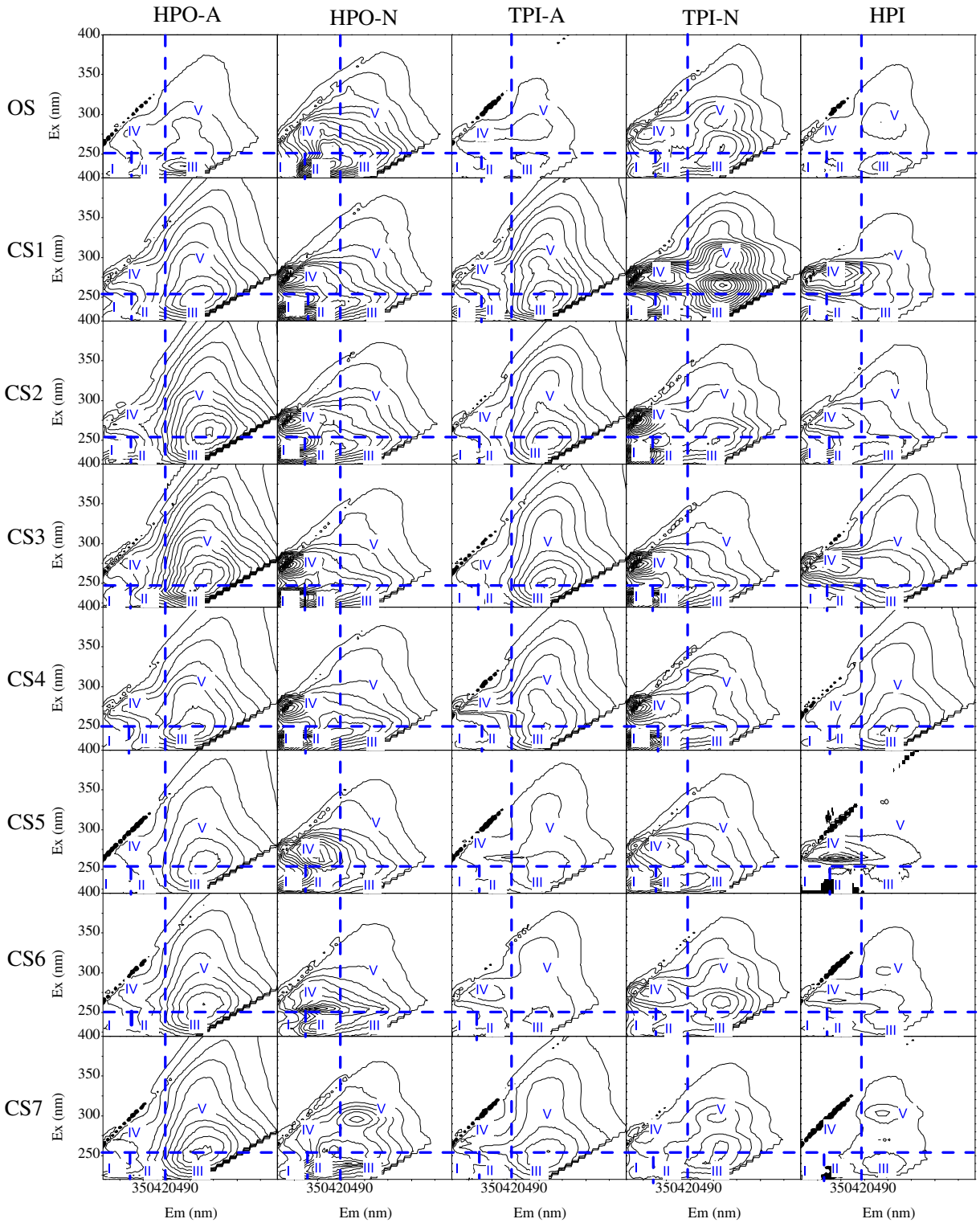

Fig. 1 EEM spectra for DOM fractions extracted from soil samples. *OS* represents the original soil used to pack the columns. *CS1*, *CS2*, *CS3*, *CS4*, *CS5*, *CS6*, and *CS7* indicate the soil layer of 0–12.5, 12.5–25, 25–50, 50–75, 75–100, 100–125, and 125–150 cm in the soil–column system, respectively. *HPO-A, HPO-N, TPI-A, TPI-N*, and *HPI* are abbreviations of hydrophobic acid, hydrophobic neutral, transphilic acid, transphilic neutral and hydrophilic fraction, respectively

Table 2 FRI parameters for operationally defined EEM regions

EEM region	No. of EEM data points per region (N)	Projected excitation–emission area (nm^2)	Fractional projected area per region	MF_i
I	287	1,435	0.039	25.64
II	350	1,750	0.048	20.83
III	553	2,765	0.075	13.33
IV	1,310	6,550	0.179	5.59
V	4,839	24,195	0.659	1.52
Summation	7,339	36,695	1.000	–

addition, TPI-N and HPI in CS1–CS4 also showed an increase in $\Phi_{T,n}$ value. These increases were significant ($p<0.05$). On the other hand, the decrease in $\Phi_{T,n}$ value may indicate the dominance of less fluorescent components in soil DOM fractions resulted from infiltration of wastewater effluents in SAT. Such decrease was seen for HPO-N, TPI-N, and HPI in CS5–CS7 ($p<0.05$). As for HPO-N in CS1–CS4, $\Phi_{T,n}$ values were close to that for the OS HPO-N. The changes in $\Phi_{T,n}$ value for soil DOM fractions in SAT might be attributed to biomass formation and organics absorption onto the soils resulted from SAT-applied wastewater effluents, as well as to dissolution of original soil organic matter (SOM), which enters the infiltrated waters.

As shown in Fig. 2, the $\Phi_{i,n}$ behavior was distinct and different for these five fractions. HPO-A in CS1–CS7 showed significantly higher values for $\Phi_{I,n}$–$\Phi_{V,n}$ than that in OS ($p<0.05$), with the exception of $\Phi_{I,n}$, $\Phi_{II,n}$, and $\Phi_{IV,n}$ in CS5 and CS6. On the contrary, only $\Phi_{I,n}$ in CS1–CS4 HPO-N was higher than the corresponding value in OS HPO-N ($p<0.05$). Except for $\Phi_{II,n}$ and $\Phi_{IV,n}$ in CS5, $\Phi_{II,n}$–$\Phi_{V,n}$ values for TPI-A in CS1–CS7 were significantly higher in comparison with that in OS ($p<0.05$). For TPI-N, $\Phi_{IV,n}$ in CS1–CS6 had higher values whereas $\Phi_{V,n}$ in CS2–CS7 had lower values, as compared to that in OS ($p<0.05$). $\Phi_{II,n}$–$\Phi_{IV,n}$ for HPI in CS1–CS4 increased in values relative to that for OS HPI, while $\Phi_{I,n}$ and $\Phi_{II,n}$ for CS5–CS7 HPI behaved contrarily ($p<0.05$).

For OS, the highest cumulative EEM volume in OS ($\Phi_{T,n}$ =9.0×108 AUnm^2L/mg) was observed in HPO-N, followed by TPI-N ($\Phi_{T,n}$=6.0×107 AUnm^2L/mg). In comparison, $\Phi_{T,n}$ values for HPO-A, TPI-A, and HPI were significantly lower ($p<0.05$), at 2.8×108, 1.9×108, and 2.0×108 AUnm^2L/mg, respectively. The results suggested that HPO-N and TPI-N were remarkably more fluorescent than the other three fractions in OS. Interestingly, $\Phi_{T,n}$ values for DOM fractions in CS1–CS7 could be ranked as follows: HPO-N and TPI-N > HPO-A > TPI-A and HPI ($p<0.05$). For all DOM fractions, the $\Phi_{I,n}$–$\Phi_{V,n}$ and $\Phi_{T,n}$ values in CS1–CS3 were higher than the corresponding values

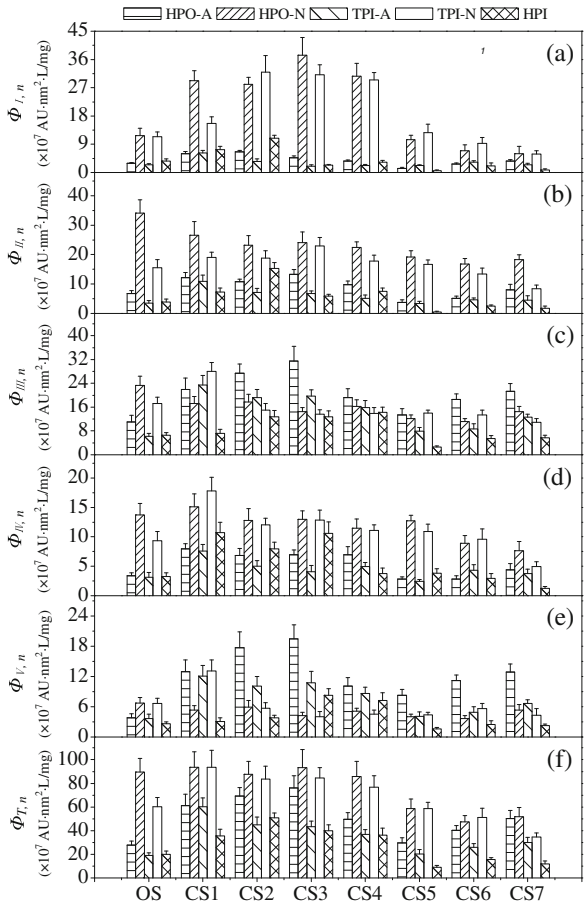

Fig. 2 $\Phi_{I,n}$ (**a**), $\Phi_{II,n}$ (**b**), $\Phi_{III,n}$ (**c**), $\Phi_{IV,n}$ (**d**), $\Phi_{V,n}$ (**e**), and $\Phi_{T,n}$ (**f**) values for DOM fractions extracted from soil samples. *OS* represents the original soil used to pack the columns. *CS1*, *CS2*, *CS3*, *CS4*, *CS5*, *CS6*, and *CS7* indicate the soil layer of 0–12.5, 12.5–25, 25–50, 50–75, 75–100, 100–125, and 125–150 cm in the soil–column system, respectively. *HPO-A, HPO-N, TPI-A, TPI-N*, and *HPI* are abbreviations of hydrophobic acid, hydrophobic neutral, transphilic acid, transphilic neutral and hydrophilic fraction, respectively. $\Phi_{i,n}$ represents normalized region-specific EEM volume, which is obtained by normalizing the volume beneath region "*i*" of the EEM to the fractional projected excitation–emission area. $\Phi_{T,n}$ indicates cumulative EEM volume, which is equal to the sum of $\Phi_{I,n}$–$\Phi_{V,n}$

in CS5–CS7, with the exception of $\Phi_{V,n}$ for CS7 HPO-N, $\Phi_{I,n}$ for CS6 TPI-A, and $\Phi_{V,n}$ for CS6 TPI-N, indicating that the upper soils were enriched in more fluorescent DOM. The DOM in top soil of 0–12.5 cm was characterized by highly efficient SMP-like fluorophores, as the highest ΦIV, *n* value for these five fractions in all soil samples occurred in CS1. Additionally, HPO-N and TPI-N in each soil sample exhibited significantly higher $\Phi_{I,n}$, $\Phi_{II,n}$, and $\Phi_{IV,n}$ values than the other three fractions ($p<0.05$), which implied that neutral fractions (i.e., HPO-N and TPI-N) in soils contained more protein-like fluorescent materials.

The distribution of volumetric fluorescence among five regions (i.e., $P_{i,n}$) was presented in Fig. 3. Both HPO-A and TPI-A in all soil samples used in this study exhibited a common general relationship with respect to $P_{i,n}$: $P_{III,n} > P_{V,n} > P_{II,n} > P_{IV,n} > P_{I,n}$, with the exception of HPO-A in OS, in which $P_{II,n}$ showed the second highest value. In each sol sample, $P_{i,n}$ values for combined regions III and V were higher than that for combined regions I, II, and IV, indicating the dominance of humic-like fluorophores over protein-like fluorophores in these two fractions. A 2-year SAT operation seemed to cause increases in content of humic-like fluorophores as well as decreases

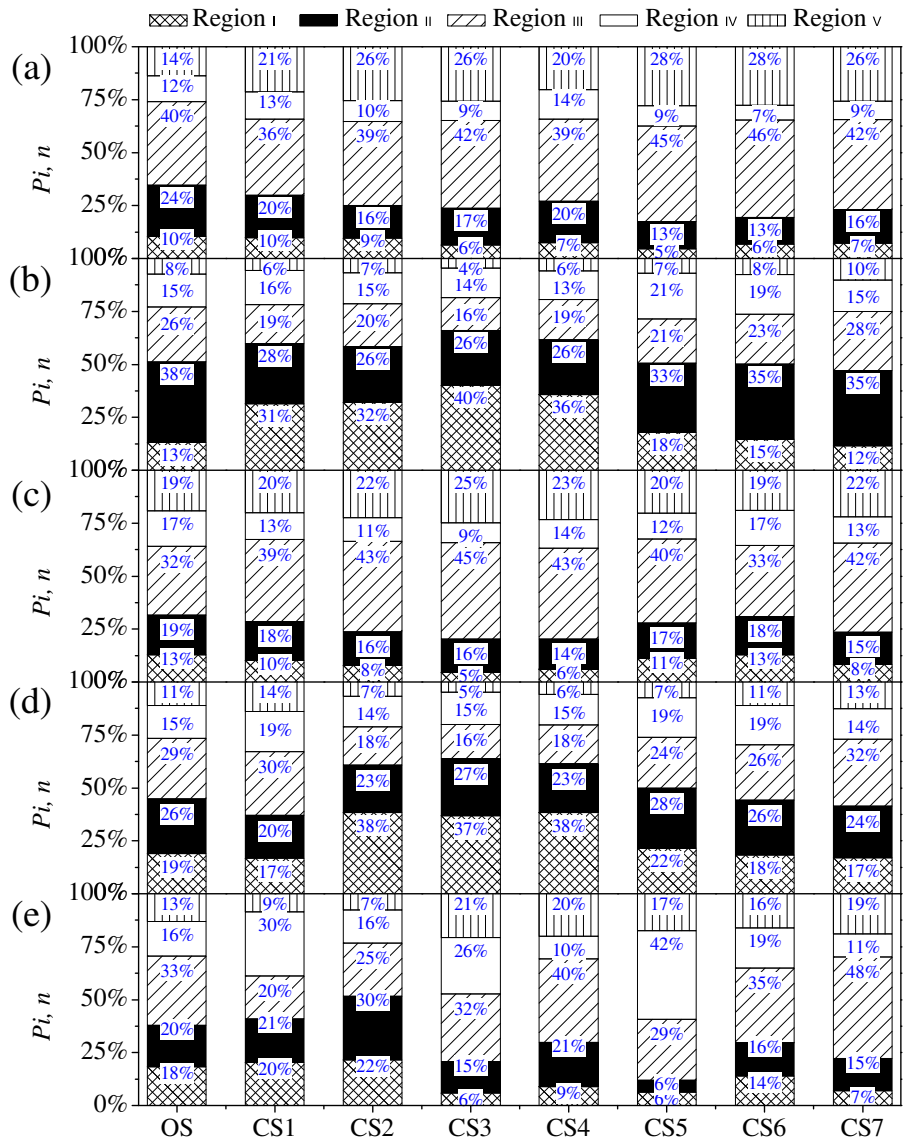

Fig. 3 Distribution of volumetric fluorescence among five regions in HPO-A (**a**), HPO-N (**b**), TPI-A (**c**), TPI-N (**d**), and HPI (**e**) extracted from soil samples. OS represents the original soil used to pack the columns. *CS1*, *CS2*, *CS3*, *CS4*, *CS5*, *CS6*, and *CS7* indicate the soil layer of 0–12.5, 12.5–25, 25–50, 50–75, 75–100, 100–125, and 125–150 cm in the soil–column system, respectively. *HPO, TPI*, and *HPI* are abbreviations of hydrophobic acid and neutral fraction, transphilic acid and neutral fraction, and hydrophilic fraction, respectively. $P_{i,n}$ indicates the percent fluorescence response, which is calculated as $\Phi_{i,n}$(normalized region−specify EEM volume)$/\Phi_{T,n}$ (cumulative *EEM* volume). ×100%

in content of protein-like fluorophores in both HPO-A and TPI-A in soils, as the sum of $P_{III,\,n}+P_{V,\,n}$ increased whereas that of $P_{I,\,n}+P_{II,\,n}+P_{IV,\,n}$ decreased in CS1–CS7 relative to OS. These increases as well as decreases were significant ($p<0.05$). Aromatic protein-like fluorophores were the predominant fluorescent materials in both HPO-N and TPI-N in all soil samples, as indicated by the significantly higher $P_{i,\,n}$ values for combined regions I and II in comparison with $P_{III,\,n}$, $P_{IV,\,n}$, and $P_{V,\,n}$ ($p<0.05$). Protein-like fluorophores, in stead of humic-like fluorophores, contributed more to the fluorescence in both HPO-N and TPI-N in each soil sample, and this was in contrary to the fluorescence results of HPO-A and TPI-A. As for HPI, however, there was not a general relationship with respect to $P_{i,\,n}$ observed.

DOC and total fluorescence of DOM fractions in soils in SAT

Based on the DOC concentration for DOM fractions extracted from soil samples used in this study shown in Fig. 4a, it could be stated that SAT operation resulted in the significantly increased amount of HPO-N, TPI-N, and HPI, as well as the significantly decreased amount of HPO-A and TPI-A in soils ($p<0.05$). Additionally, the highest DOC concentration for HPO-N, TPI-N, and HPI was observed to occur in CS1. Fox et al. (2005) reported an accumulation of biomass and associated organic matter in the surface soil in SAT. Thus, it was concluded that the accumulation of organics in the surface soil was mainly attributed to enrichment of HPO-N, TPI-N, and HPI resulted from infiltration of wastewater effluent in SAT.

Total $\Phi_{T,\,n}$ values for DOM fractions in OS and CS1–CS7 shown in Fig. 4b, which was calculated as $\Phi_{T,\,n}$ (DOC-normalized cumulative EEM volume in Fig. 2)×DOC, representing the amount of fluorescent materials in these fractions. HPO-A, HPO-N, TPI-A, TPI-N, and HPI in OS had a total $\Phi_{T,\,n}$ value of 1.4×10^9, 1.5×10^9, 6.8×10^8, 6.9×10^8, and 3.8×10^8 AU nm^2, respectively. After a 2-year SAT operation, total $\Phi_{T,\,n}$ values for these five fractions in CS1 increased by 42, 100, 116, 249, and 297 %, respectively. By comparison of both DOC-normalized $\Phi_{T,\,n}$ and DOC for DOM fractions in OS and CS1, it was suggested that the remarkable increased total $\Phi_{T,\,n}$ values for HPO-A and TPI-A in CS1 was primarily attributed to the increase in DOC-normalized $\Phi_{T,\,n}$, which represented the efficiency of fluorophores, while that for HPO-N, TPI-N, and HPI in CS1 was mainly due to the increase in DOC concentration. Although HPO-A, HPO-N, TPI-A, TPI-N, and HPI in CS2–CS4 exhibited increases of 17–67, 11–36, 46–82, 65–115, and 170–356 % in total $\Phi_{T,\,n}$ relative to those in OS, the total $\Phi_{T,\,n}$ values for each fraction in CS5–CS7

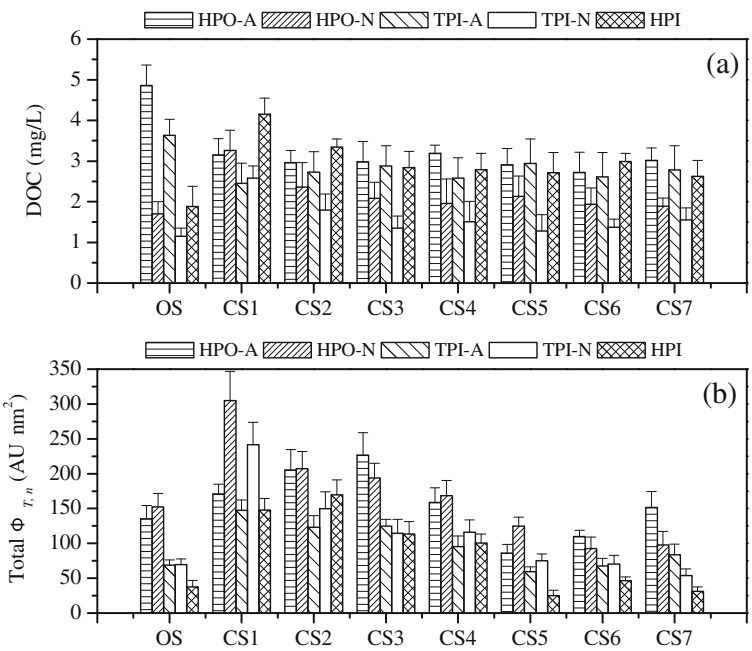

Fig. 4 DOC (**a**) and total $\Phi_{T,\,n}$ (**b**) values for DOM fractions extracted from soil samples. *OS* represents the original soil used to pack the columns. *CS1*, *CS2*, *CS3*, *CS4*, *CS5*, *CS6*, and *CS7* indicate the soil layer of 0–12.5, 12.5–25, 25–50, 50–75, 75–100, 100–125, and 125–150 cm in the soil–column system, respectively. *HPO-A, HPO-N, TPI-A, TPI-N*, and *HPI* are abbreviations of hydrophobic acid, hydrophobic neutral, transphilic acid, transphilic neutral and hydrophilic fraction, respectively. Total $\Phi_{T,\,n}$ represents the amount of fluorescent materials, which is obtained by multiplying $\Phi_{T,\,n}$ (cumulative EEM volume) by the DOC concentration

were significantly lower than those in CS1–CS4 ($p<0.05$), suggesting an accumulation of fluorescent organic matter in the upper 75 cm of soil as a consequence of SAT operation.

As shown in Fig. 5a, HPO-A was found to be the most abundant fraction in OS, constituting 37 % of the DOC. TPI-A was the second most dominant fraction, accounting for 27 %. These two fractions collectively accounted for more than 64 % of their DOM as DOC. Thus, DOM in OS is primarily acidic. On the other hand, HPO-N, TPI-N, and HPI in this soil sample were found in minority, with a percentage of 13, 9, and 14 %, respectively. After a 2-year SAT operation, the post-SAT soil increased in the relative contents of HPO-N, TPI-N, and HPI and decreased in the relative contents of HPO-A and TPI-A as compared with the pre-SAT soil, as indicated by the percentages of 20–27, 16–21, 16–25, 11–17, and 22–17 % made up by HPO-A, HPO-N, TPI-A, TPI-N, and HPI in CS1–CS7, respectively. These increases in the relative contents of HPO-N, TPI-N, and HPI, as well as decreases in the relative contents of HPO-A and TPI-A were significant ($p<0.05$).

HPO-N was the major contributor to the total fluorescence in OS (33 %), while HPO-A was the second (29 %; Fig. 5b). TPI-A, TPI-N, and HPI were relatively minor, contributing 15, 15, and 8 % of the total fluorescence in this soil sample, respectively. For CS1, HPO-N, and TPI-N accounted for 30 and 24 % of the total fluorescence, respectively; the percentages of the total fluorescence in CS1 corresponding to HPO-A, TPI-A, and HPI were comparable at 17, 15, and 15 %, respectively. The distribution of total fluorescence among five DOM fractions in CS2–CS7 was similar to that in OS: HPO-A and HPO-N were the two major fractions that contributed fluorescence, corresponding to 23–36 % and 23–34 % of the total fluorescence; the other three fractions were responsible for the remaining 42–52 % of the total fluorescence and each accounted for less than 20 %. It was noticed that the percentages of DOC made up by HPO-N and TPI-N were lower than the corresponding portions of the total fluorescence in almost all soil samples, and this was contrary to the results of TPI-A and HPI, suggesting that HPO-N and TPI-N were more fluorescent and TPI-A and HPI were less fluorescent than organics (on average) that comprise DOC in soils.

Synchronous fluorescence spectra of DOM fractions in soils in SAT

The synchronous fluorescence spectra generated for DOM fractions extracted from eight soil samples were presented in Fig. 6. Based on these maps, three main synchronous fluorescence peaks, not necessarily occurring in all spectra, were identified. Peak 1 at

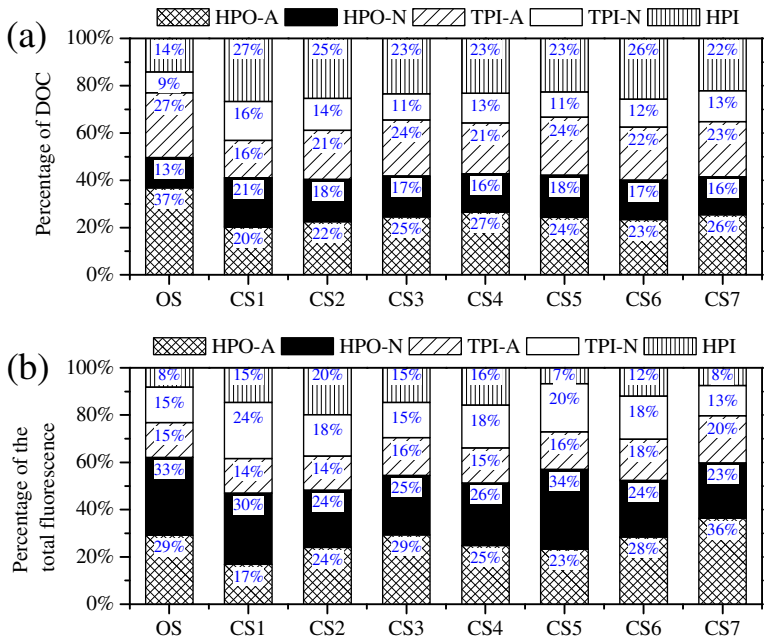

Fig. 5 Distribution of DOC (**a**) and total fluorescence (**b**) among five DOM fractions extracted from soil samples. *OS* represents the original soil used to pack the columns. *CS1*, *CS2*, *CS3*, *CS4*, *CS5*, *CS6*, and *CS7* indicate the soil layer of 0–12.5, 12.5–25, 25–50, 50–75, 75–100, 100–125, and 125–150 cm in the soil–column system, respectively. *HPO-A, HPO-N, TPI-A, TPI-N*, and *HPI* are abbreviations of hydrophobic acid, hydrophobic neutral, transphilic acid, transphilic neutral and hydrophilic fraction, respectively

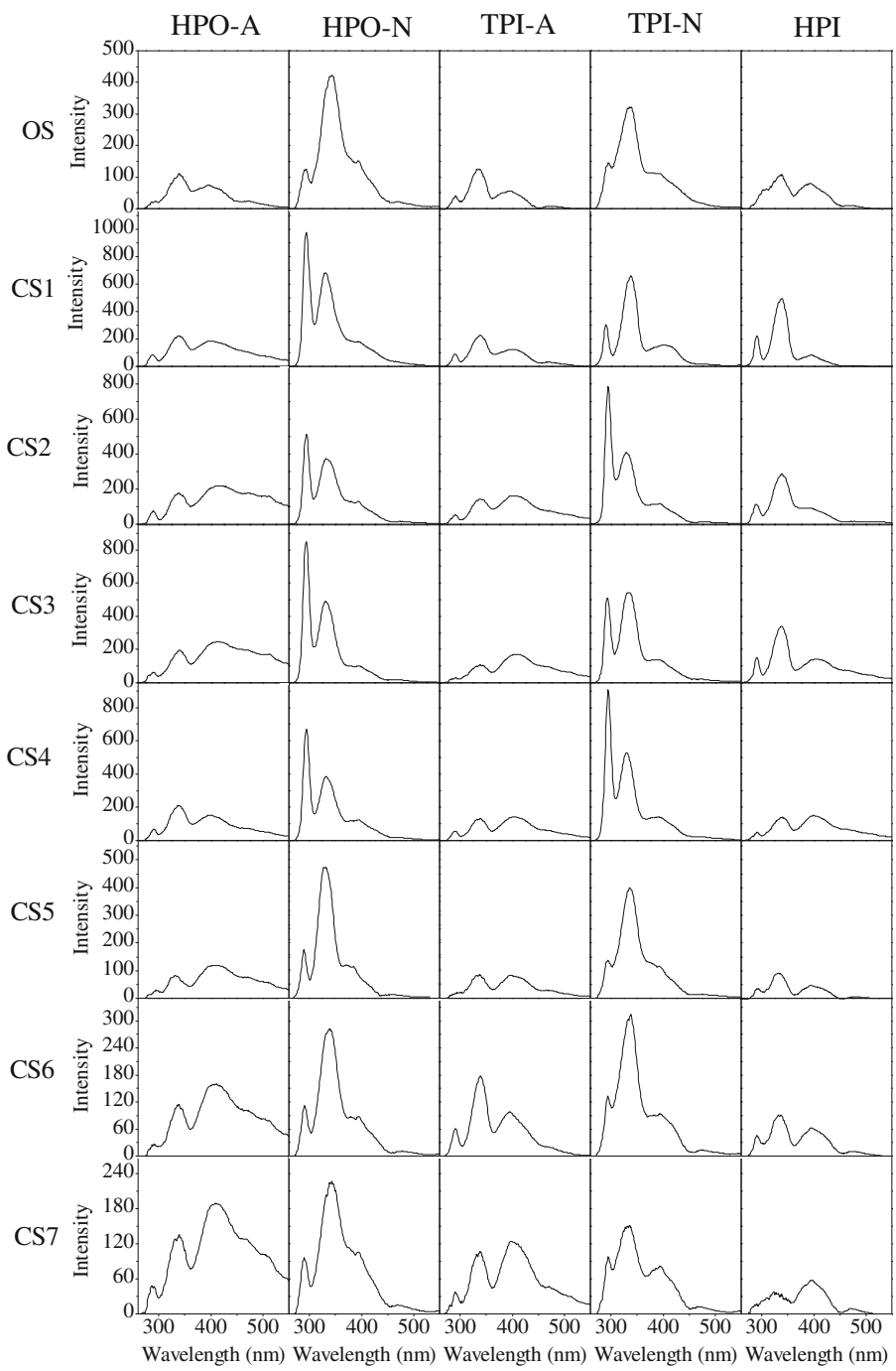

Fig. 6 Synchronous fluorescence spectra for DOM fractions extracted from soil samples (Δλ=60 nm). *OS* represents the original soil used to pack the columns. *CS1*, *CS2*, *CS3*, *CS4*, *CS5*, *CS6*, and *CS7* indicate the soil layer of 0–12.5, 12.5–25, 25–50, 50–75, 75–100, 100–125, and 125–150 cm in the soil–column system, respectively. *HPO-A, HPO-N, TPI-A, TPI-N*, and *HPI* are abbreviations of hydrophobic acid, hydrophobic neutral, transphilic acid, transphilic neutral and hydrophilic fraction, respectively

290–300 nm and peak 2 at 330–340 nm were located in the shoulder ranges of SMP- and humic acid-like fluorophores, respectively, as compared with EEM spectra. Peak 3 at 395–415 nm might be indicative of the presence of polycyclic aromatic structures like flavone and coumarine (with Ex/Em of 400–420/460–480 nm) (Zhang et al. 2008). Thus, the existence of SMP- and humic acid-like components and polycyclic aromatic compounds in SOM in SAT, which were "hidden" in EEM spectra, was illustrated by synchronous fluorescence spectra.

For each soil sample, HPO-N and TPI-N exhibited significantly stronger peaks of 1 and 2 than the other three fractions thus indicating higher content of fluorescent

materials corresponding to peaks of 1 and 2 in these two fractions (Fig. 6). On the other hand, the strongest peak 3 corresponded to HPO-A in all soil samples of CS1–CS7. Moreover, the peak 3 of HPO-A was always red-shifted relative with the other fractions, suggesting a higher degree of polycondensation and humification of fluorophores responsible for peak 3 in this fraction.

As shown in Fig. 6, each fraction in CS1 had an increased intensity for peaks of 1–3 relative to that in OS. In addition, it was also noticed that both peaks 1 and 2 in each fraction in CS1, with the exception of peak 1 in TPI-N, exhibited higher intensity than those in all the other soil samples. The results implied that SAT operation resulted in the enrichment of fluorescent materials corresponding to these three synchronous peaks in the surface soil (0–12.5 cm), which were probably related to an accumulation of biomass and associated organic matter (Fox et al. 2005).

Conclusions

The aim of this work was to investigate changes in the fluorescence characteristics of soil DOM fractions during SAT. The following conclusions are drawn on the basis of the experimental results:

1 $\Phi_{T,\,n}$ values for DOM fractions in all soil samples could be ranked as follows: HPO-N and TPI-N > HPO-A > TPI-A and HPI. A 2-year SAT operation resulted in the enrichment of more fluorescent components in HPO-A and TPI-A in soils, as well as the dominance of less fluorescent components in HPO-N, TPI-N, and HPI in the bottom soil (75–150 cm).
2 The change trend of $\Phi_{i,\,n}$ was distinct and different for DOM fractions along the soil profile in the soil columns.
3 Total $\Phi_{T,\,n}$ values for DOM fractions in soils suggested an accumulation of fluorescent organic matter in the upper 75 cm of soil as a consequence of SAT operation.
4 The synchronous fluorescence spectra revealed the presence of SMP- and humic acid-like components and polycyclic aromatic compounds in SOM in SAT, and SAT operation led to the enrichment of fluorescent materials corresponding to synchronous peaks exhibiting fluorescence signals at 290–300, 330–340, and 395–415 in all DOM fractions in the surface soil (0–12.5 cm).

Acknowledgments The work was supported by the National Natural Science Foundation of China (no. 21107039), the Science and Technology Research Program of Educational Committee of Liaoning Province (no. 201203), the Planned Science and Technology Project of Liaoning Province (no. 2011230009), and the Key Discipline Foundation of Liaoning Province.

References

Aiken, G. L., McKnight, D. M., Thorn, K. A., & Thurman, E. M. (1992). Isolation of hydrophilic organic acids from water using nonionic macroporous resins. *Organic Geochemistry, 18*(4), 567–573.

Akagi, J., Zsolnay, A., & Bastida, F. (2007). Quantity and spectroscopic properties of soil dissolved organic matter (DOM) as a function of soil sample treatments: air-drying and pre-incubation. *Chemosphere, 69*(7), 1040–1046.

Amy, G., & Drewes, J. (2007). Soil aquifer treatment (SAT) as a natural and sustainable wastewater reclamation/reuse technology: fate of wastewater effluent organic matter (EfOM) and trace organic compounds. *Environmental Monitoring and Assessment, 129*(1–3), 19–26.

Barber, L. B., Leenheer, J. A., Noyes, T. I., & Stiles, E. A. (2001). Nature and transformation of dissolved organic matter in treatment wetlands. *Environmental Science and Technology, 35*(24), 4805–4816.

Boehme, J., Coble, P., Conmy, R., & Stovall-Leonard, A. (2004). Examining CDOM fluorescence variability using principal component analysis: seasonal and regional modeling of three-dimensional fluorescence in the Gulf of Mexico. *Marine Chemistry, 89*(1–4), 3–14.

Chen, J., LeBoeuf, E. J., Dai, S., & Gu, B. (2003). Fluorescence spectroscopic studies of natural organic matter fractions. *Chemosphere, 50*(5), 639–647.

Chen, W., Westerhoff, P., Leenheer, J. A., & Booksh, K. (2003). Fluorescence excitation–emission matrix regional integration to quantify spectra for dissolved organic matter. *Environmental Science and Technology, 37*(24), 5701–5710.

Chow, A. T., Guo, F., Gao, S., & Breuer, R. S. (2006). Size and XAD fractionations of trihalomethane precursors from soils. *Chemosphere, 62*(10), 1636–1646.

Drewes, J. E., Quanrud, D. M., Amy, G. L., & Westerhoff, P. K. (2006). Character of organic matter in soil–aquifer treatment systems. *Journal of Environmental Engineering ASCE, 132*(11), 1447–1458.

Embacher, A., Zsolnay, A., Gattinger, A., & Munch, J. C. (2007). The dynamics of water extractable organic matter (WEOM) in common arable topsoils: I. Quantity, quality and function over a three year period. *Geoderma, 139*(1–2), 11–22.

Fox, P., Aboshanp, W., & Alsamadi, W. (2005). Analysis of soils to demonstrate sustained organic carbon removal during soil aquifer treatment. *Journal of Environmental Quality, 34*(1), 156–163.

Juhna, T., Klavins, M., & Eglite, L. (2003). Sorption of humic substances on aquifer material at artificial recharge of groundwater. *Chemosphere, 51*(9), 861–868.

Leenheer, J. A., & Croué, J. P. (2003). Characterizing aquatic dissolved organic matter. *Environmental Science and Technology, 37*(1), 18A–26A.

Marhuenda-Egea, F. C., Martínez-Sabater, E., Jordá, J., Moral, R., Bustamante, M. A., Paredes, C., et al. (2007). Dissolved organic matter fractions formed during composting of winery and distillery residues: evaluation of the process by fluorescence excitation–emission matrix. *Chemosphere, 68*(2), 301–309.

Ohno, T., Fernandez, I. J., Hiradate, S., & Sherman, J. F. (2007). Effects of soil acidification and forest type on water soluble soil organic matter properties. *Geoderma, 140*(1–2), 176–187.

Peuravuori, J., Koivikko, R., & Pihlaja, K. (2002). Characterization, differentiation and classification of aquatic humic matter separated with different sorbents: synchronous scanning fluorescence spectroscopy. *Water Research, 36*(18), 4552–4562.

Quanrud, D. M., Arnold, R. G., Wilson, L. G., Gordon, H. J., Graham, D. M., & Amy, G. L. (1996). Fate of organics during column studies of soil aquifer treatment. *Journal of Environmental Engineering ASCE, 122*(4), 314–321.

Quanrud, D. M., Hafer, J., Karpiscak, M. M., Zhang, J., Lansey, K. E., & Arnold, R. G. (2003). Fate of organics during soil–aquifer treatment: sustainability of removals in the field. *Water Research, 37*(14), 3401–3411.

Rauch, T., & Drewes, J. E. (2005). Quantifying organic carbon removal in groundwater recharge systems. *Journal of Environmental Engineering ASCE, 131*(6), 909–923.

Sierra, M. M. D., Giovanela, M., Parlanti, E., & Soriano-Sierra, E. J. (2005). Fluorescence fingerprint of fulvic and humic acids from varied origins as viewed by single-scan and excitation/emission matrix techniques. *Chemosphere, 58*(6), 715–733.

Westerhoff, P., & Pinney, M. (2000). Dissolved organic carbon transformations during laboratory-scale groundwater recharge using lagoon-treated wastewater. *Waste Management, 20*(1), 75–83.

Xiao, X., Zhang, Y. J., Wang, Z. G., Jin, D., Yin, G. F., & Zhao, N. J. (2010). Experimental studies on three-dimensional fluorescence spectral of mineral oil in ethanol. *Spectroscopy and Spectral Analysis, 30*(6), 1549–1554.

Xue, S., Zhao, Q. L., Wei, L. L., Wang, L. N., & Liu, Z. G. (2007). Fate of secondary effluent dissolved organic matter during soil–aquifer treatment. *Chinese Science Bulletin, 52*(18), 2496–2505.

Xue, S., Zhao, Q. L., Wei, L. L., & Ren, N. Q. (2009). Behavior and characteristics of dissolved organic matter during column studies of soil aquifer treatment. *Water Research, 43*(2), 499–507.

Zepp, R. G., Sheldon, W. M., & Moran, M. A. (2004). Dissolved organic fluorophores in southeastern US coastal waters: correction method for eliminating Rayleigh and Raman scattering peaks in excitation–emission matrices. *Marine Chemistry, 89*(1–4), 15–36.

Zhang, T., Lu, J. F., Ma, J., & Qiang, Z. M. (2008). Fluorescence spectroscopic characterization of DOM fractions isolated from a filtered river water after ozonation and catalytic ozonation. *Chemosphere, 71*(5), 911–921.